Inversion for reservoir parameters using first- and second-order derivatives of elastic impedance

Huaizhen Chen* and Kristopher A. Innanen

ABSTRACT

Estimation of reservoir porosity, shale content and fluid type is the key and difficult problem of geophysical exploration. Based on rock physics theory and effective models, we relate seismic reflection coefficient and elastic impedance (EI) to reservoir porosity, shale content and fluid. Using the nonlinear reflection coefficient and EI, we present a two-step inversion method, which involves: 1) linear inversion of partially incidence-angle-stacked data to predict EI; and 2) nonlinear inversion of EI to estimate shale content, porosity, fluid modulus and density. We introduce the procedure of using the first- and second-order derivatives of EI to improve the accuracy of the inversion. The robustness and reliability of the proposed inversion method are verified using noisy synthetic seismic datasets and real data.

INTRODUCTION

Prediction of reservoir parameters (shale content, porosity) and identification of fluid type are crucial to characterization of reservoirs. Through seismic inversion, geophysicists first estimate elastic parameters (e.g. velocity, Lamé constants) from seismic amplitude data, and then convert the estimated elastic parameters to reservoir parameters based on rock physics effective models. A method of direct inversion for reservoir parameters and fluid factors using seismic data is required.

Currently, the commonly used fluid factors are mainly established based on difference between bulk moduli of water and gas (water: 2.865 GPa; gas: 0.041 GPa). The fluid substitution model, proposed by Gassmann (1951), is used to analyze effects of different fluids on rock elastic properties (e.g. bulk and shear moduli, P- and S-wave velocities, Lamé constants, Poisson's ratio, etc.). Geophysicists propose a series of fluid indicators by combining various parameters related to fluid type and content. Russell et al. (2003) propose a fluid indicator (fluid/porosity term) based on the fluid substitution model. However, the constructed fluid/porosity term is indeed influenced by the comprehensive influence of lithology, fluid and porosity, which reduces the sensitivity to fluid. Chen and Zhang (2017) present the fluid/porosity term is much more affected by porosity than by fluids, and may have certain limitations in practical applications. In this study, we use fluid bulk modulus, which is only related to fluid type and content, as an indicator.

Parameterization of reflection coefficient is the basis of pre-stacked seismic inversion. Aki and Richards (1980) propose a linearized reflection coefficient in terms of reflectivities of P- and S-wave velocities and density. Goodway et al. (1997) present a linearized reflection coefficient that is expressed as a function of Lamé parameters and density. Based

*School of Ocean and Earth Science, Tongji University, Shanghai, China; and CREWES Project, University of Calgary, Calgary, Alberta, Canada. Email: huaizhen.chen@ucalgary.ca

on the fluid substitution model, Russell et al. (2003, 2011) propose reflection coefficient expressed in terms of fluid factor, which relates the fluid information to seismic amplitude directly. However, there is no an explicit reflection coefficient that can relate reservoir parameters and fluid indicator to pre-stacked seismic amplitudes.

In this study, we derive the reflection coefficient and elastic impedance (EI) that are expressed as a function of reservoir parameters (shale content, porosity) and fluid factor (fluid bulk modulus) based on rock physics effective models. Using the derived reflection coefficient and EI, we propose an inversion method of employing pre-stacked seismic amplitudes to estimate reservoir parameters. We employ noisy synthetic and real data sets to verify that the proposed inversion method is robust, and we may obtain reliably estimated results of reservoirs parameters using the proposed inversion method.

THEORY AND METHOD

In this section, we present the derivation of EI that is a function of reservoir parameters and the method of estimating reservoir parameters using first- and second-order derivatives of EI.

Elastic impedance parameterized in terms of reservoir parameters

The fluid substitution model, proposed by Gassmann (1951), is employed to calculate bulk and shear moduli of saturated rock (K_{sat} and μ_{sat}) using bulk and shear moduli of dry rock (K_{dry} and μ_{dry}), porosity (ϕ) and fluid bulk modulus (K_f)

$$K_{\mathrm{sat}} = K_{\mathrm{dry}} + \frac{\left(1 - K_{\mathrm{dry}}/K_0\right)^2}{\phi/K_{\mathrm{f}} + \left(1-\phi\right)/K_0 - K_{\mathrm{dry}}/K_0^2},$$

$$\mu_{\mathrm{sat}} = \mu_{\mathrm{dry}}, \tag{1}$$

where K_0 is bulk modulus of minerals that make up the rock.

Krief et al. (1990) proposed an approximate relationship between bulk and shear moduli of dry rock and porosity, which is given by

$$K_{\mathrm{dry}} = K_0 M\left(\phi\right),$$

$$\mu_{\mathrm{dry}} = \mu_0 M\left(\phi\right), \tag{2}$$

where μ_0 is shear modulus of minerals that make up the rock, and

$$M\left(\phi\right) = \left(1-\phi\right)^{\frac{3}{1-\phi}} \approx 1 - 3\phi + \frac{7}{2}\phi^3. \tag{3}$$

In the case of fluid-saturated reservoirs, we may simplify the bulk and shear moduli of saturated rock as

$$K_{\mathrm{sat}} \approx K_0\, M\left(\phi\right) + \frac{\left[1 - M\left(\phi\right)\right]^2}{\phi/K_{\mathrm{f}}}$$

$$\approx K_0\, M\left(\phi\right) + K_f\, F\left(\phi\right),$$

$$\mu_{\text{sat}} = \mu_0 \, M\left(\phi\right), \tag{4}$$

where

$$F\left(\phi\right) \approx \phi \left(3 - \frac{7}{2}\phi^2\right)^2 . \tag{5}$$

Under assumptions of quartz and shale making up the rock, we employ the Voigt-Reuss-Hill average model to calculate K_0 and μ_0 as

$$\begin{aligned} K_0 = Y_1\left(V_c\right) &= \frac{1}{2}\left[K_q + \left(K_c - K_q\right)V_c + \frac{K_q K_c}{K_c + \left(K_q - K_c\right)V_c}\right], \\ \mu_0 = Y_2\left(V_c\right) &= \frac{1}{2}\left[\mu_q + \left(\mu_c - \mu_q\right)V_c + \frac{\mu_q \mu_c}{\mu_c + \left(\mu_q - \mu_c\right)V_c}\right], \end{aligned} \tag{6}$$

where V_c represents the shale content, $K_q = 33.6$ GPa and $\mu_q = 45$ GPa are bulk and shear moduli of quartz, and $K_c = 21$ GPa and $\mu_c = 7$ GPa are bulk and shear moduli of shale, respectively.

Gray et al. (1999) present a linearized PP-wave reflection coefficient in terms of bulk and shear moduli of saturated rock as

$$\begin{aligned} R_{PP}\left(\theta\right) = &\left(\frac{1}{4} - \frac{1}{3}\gamma_{sat}\right)\sec^2\theta \frac{\Delta K_{sat}}{K_{sat}} + \gamma_{sat}\left(\frac{1}{3}\sec^2\theta - 2\sin^2\theta\right)\frac{\Delta \mu_{sat}}{\mu_{sat}} \\ &+ \left(\frac{1}{2} - \frac{1}{4}\sec^2\theta\right)\frac{\Delta\rho}{\rho}, \end{aligned} \tag{7}$$

where $\gamma_{sat} = \mu_{sat} / \left(K_{sat} + \frac{4}{3}\mu_{sat}\right)$.

Combining equations 1-7, we derive the PP-wave reflection coefficient as a function of shale content, porosity, fluid bulk modulus and density as

$$\begin{aligned} R_{PP}\left(\theta\right) = &P_1\left(\theta\right)\frac{\Delta Y_1\left(V_c\right)}{Y_1\left(V_c\right)} + P_2\left(\theta\right)\frac{\Delta Y_2\left(V_c\right)}{Y_2\left(V_c\right)} \\ &+ P_3\left(\theta\right)\frac{\Delta F\left(\phi\right)}{F\left(\phi\right)} + P_4\left(\theta\right)\frac{\Delta M\left(\phi\right)}{M\left(\phi\right)} \\ &+ P_5\left(\theta\right)\frac{\Delta K_f}{K_f} + P_6\left(\theta\right)\frac{\Delta\rho}{\rho}, \end{aligned} \tag{8}$$

where $\gamma_{dry} = \mu_{dry} / \left(K_{dry} + \frac{4}{3}\mu_{dry}\right)$, and

$$P_1\left(\theta\right) = \frac{1}{4}\left(\frac{\gamma_{sat}}{\gamma_{dry}} - \frac{4}{3}\gamma_{sat}\right)\sec^2\theta,$$

$$P_2\left(\theta\right) = \gamma_{sat}\left(\frac{1}{3}\sec^2\theta - 2\sin^2\theta\right),$$

$$\begin{aligned}
P_3(\theta) &= \frac{1}{4}\left(1-\frac{\gamma_{sat}}{\gamma_{dry}}\right)\sec^2\theta, \\
P_4(\theta) &= \frac{1}{4}\left(\frac{\gamma_{sat}}{\gamma_{dry}}\sec^2\theta-8\gamma_{sat}\sin^2\theta\right), \\
P_5(\theta) &= P_3(\theta)=\frac{1}{4}\left(1-\frac{\gamma_{sat}}{\gamma_{dry}}\right)\sec^2\theta, \\
P_6(\theta) &= \frac{1}{2}-\frac{1}{4}\sec^2\theta,
\end{aligned} \tag{9}$$

Using the derived PP-wave reflection coefficient, we may write PP-wave EI as

$$\begin{aligned}
EI(\theta) = &\left[Y_1(V_c)\right]^{2P_1(\theta)}\left[Y_2(V_c)\right]^{2P_2(\theta)} \\
&\left[F(\phi)\right]^{2P_3(\theta)}\left[M(\phi)\right]^{2P_4(\theta)} \\
&\left(K_f\right)^{2P_5(\theta)}(\rho)^{2P_6(\theta)}.
\end{aligned} \tag{10}$$

Inversion for reservoir parameters using derivatives of EI

To obtain results of reservoir parameters from input seismic datasets, we present a two-stage inversion method. In the first stage, we implement a linear inversion of partially incidence-angle-stacked seismic data for estimating EI, and in the second stage, we use the estimated EI to predict reservoir parameters.

The damping least-squares (DLS) algorithm, which is proposed by Chen et al. (2020), is used in the estimation EI from seismic data. In this study, we focus on the second-stage inversion, i.e. the inversion of EI for reservoir parameters. In equation 10, we observe the relationship between EI and reservoir parameters is nonlinear. We succinctly express the nonlinear relationship between the vector of EI ($\mathbf{d}$) and the vector of unknown parameters ($\mathbf{m}$) as

$$\mathbf{d}=\mathbf{G}(\mathbf{m}), \tag{11}$$

where $\mathbf{G}$ represents the forwarding vector. In the case of n layer and the incidence angle θ_i, we express $\mathbf{d}$ and $\mathbf{m}$ as

$$\mathbf{d}=\begin{bmatrix} EI_1(\theta_i) \\ \vdots \\ EI_n(\theta_i) \end{bmatrix},$$

$$\mathbf{m} = \begin{bmatrix} V_c^1 \\ \vdots \\ V_c^n \\ \phi_1 \\ \vdots \\ \phi_n \\ K_f^1 \\ \vdots \\ K_f^n \\ \rho_1 \\ \vdots \\ \rho_n \end{bmatrix}, \tag{12}$$

The Newton algorithm is utilized to solve the nonlinear problem, and the vector of unknown parameters is given by

$$\mathbf{m}_{k+1} = \mathbf{m}_k + \Delta\mathbf{m}_k, \tag{13}$$

where $\mathbf{m}_k$ represents the estimated vector of unknown parameter after the kth iteration, and the update $\Delta\mathbf{m}_k$ is calculated as

$$\Delta\mathbf{m}_k = -\mathbf{H}^{-1}\mathbf{g}, \tag{14}$$

where

$$\mathbf{g} = \frac{\partial EI}{\partial \mathbf{m}}\bigg|_{\mathbf{m}=\mathbf{m}_k} \Delta\mathbf{d},$$

$$\mathbf{H} \approx \mathbf{g}\,\mathbf{g}^T, \tag{15}$$

where $\Delta\mathbf{d}$ represents difference between vectors of modeled and input EI datasets.

NUMERICAL EXAMPLES

In this section, we use synthetic and real seismic data to validate that the proposed inversion method is robust and may make reliable estimation of reservoir parameters.

Synthetic data

We first apply the proposed inversion method to synthetic data generated using a well log model. Given a Ricker wavelet of dominant frequency of 20 Hz, we generate synthetic data based on the derived reflection coefficient and the convolution model. Adding Gaussian random noise to synthetic data, we obtain the noisy seismic data of signal-to-noise ratio of 5 and 2, which serves the input data for the estimation of EI. In Figure 1, we show curves of porosity ϕ, shale content V_c, water saturation S_w and density ρ; and we also show curves of K_f, K_{dry}, K_{sat} and μ_{sat} that are calculated using the fluid substitution model and the Voigt-Reuss-Hill average model.

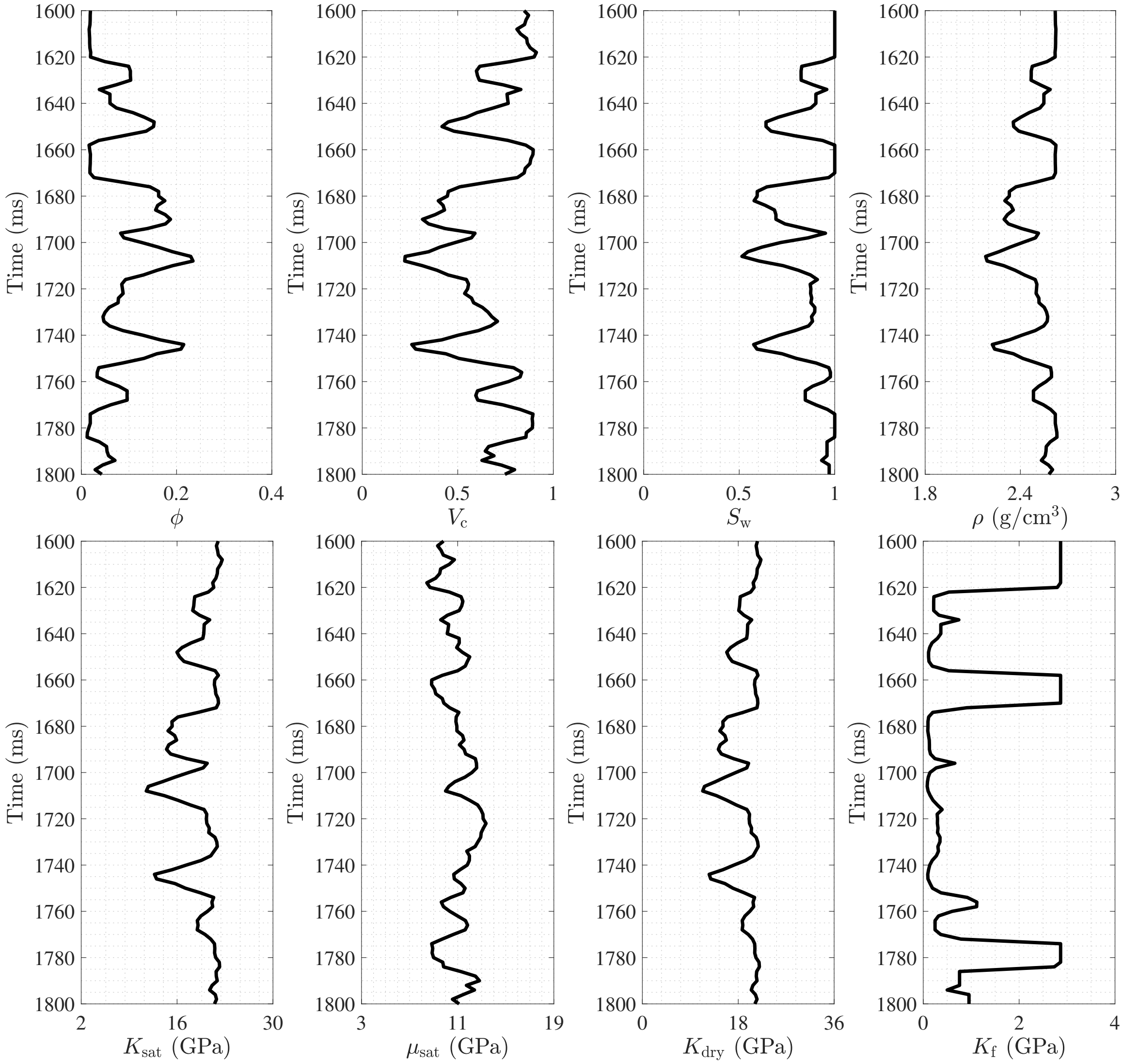

FIG. 1. Well log model.

Given angles of incidence $\theta_1 = 5°$, $\theta_2 = 12°$, $\theta_3 = 19°$ and $\theta_4 = 26°$, we show the generated noisy seismic data of signal-to-noise ratio of 5 and 2 in Figure 2. Comparisons between true values calculated using the derived EI equation and inversion results of EI obtained using the DLS algorithm are shown in Figure 3. We observe there is a good match between the inversion result and true value of EI, which illustrates the inversion result of EI can be used for the estimation of reservoir parameters in the second-stage inversion.

Using the inversion result of EI as the input, we proceed to the estimation of reservoir parameters based on the proposed nonlinear inversion method. In Figure 4, we show comparisons between inversion results and true values of V_c, ϕ, K_f and ρ. With inversion results of EI of four incidence angles, i.e. $EI\,(\theta_1)$, $EI\,(\theta_2)$, $EI\,(\theta_3)$ and $EI\,(\theta_4)$, in hand, we may obtain four sets of inversion results for each reservoir parameter, and we calculate the average of four sets of inversion results as the final inversion result of reservoir parameter.

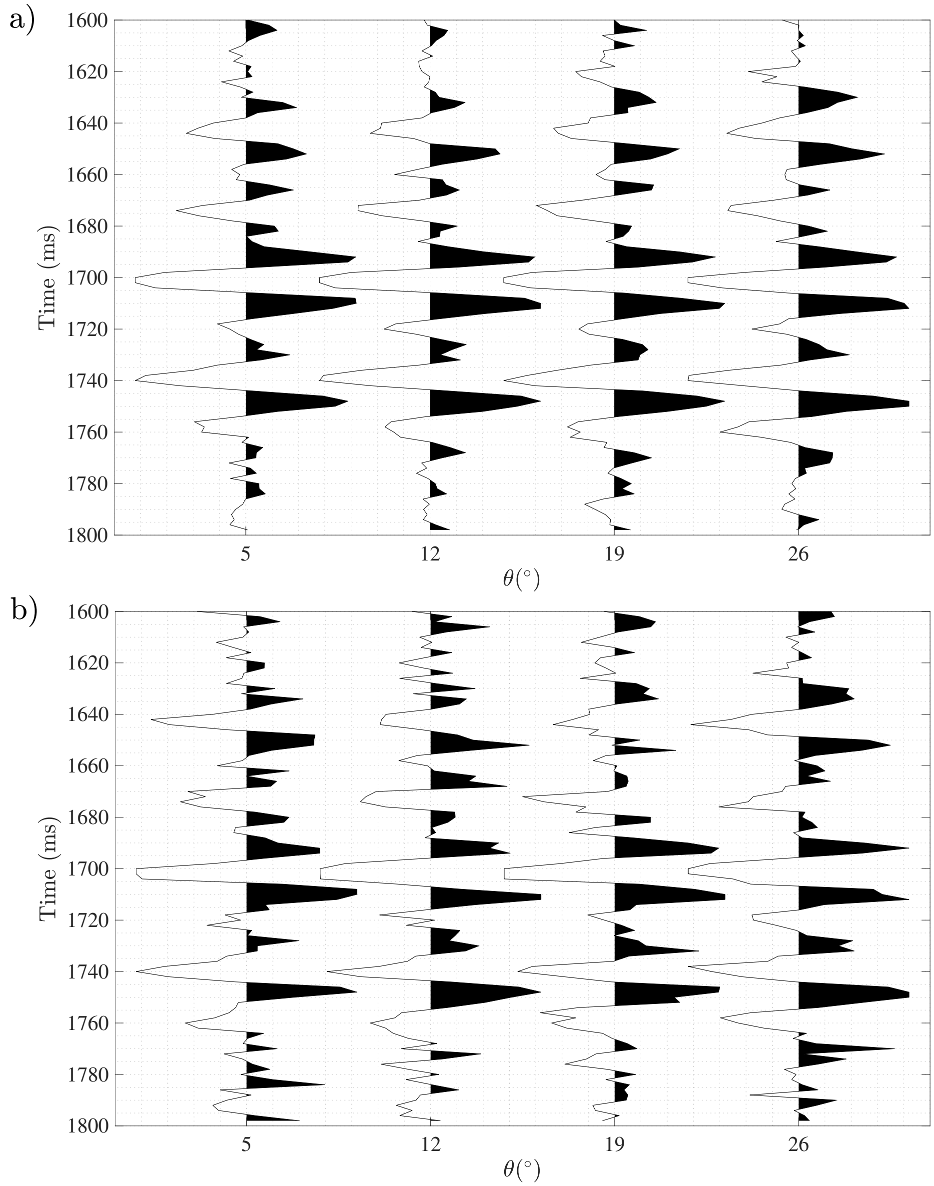

FIG. 2. Noisy seismic data. a) Signal-to-noise ratio of 5; and b) Signal-to-noise ratio of 2.

In Figure 4, we observe the final inversion result of each reservoir parameter matches the corresponding true value well. It illustrates that the proposed inversion method can be used to estimate reservoir parameters reliably from the inversion results of EI even in the case of signal-to-noise ratio of 2, which verifies the robustness of the proposed nonlinear inversion method.

Real data

We apply the proposed inversion method to a real data set acquired over a gas-bearing reservoir. Following the workflow of two-stage inversion, we first implement the inversion for EI using partially incidence-angle-stacked seismic data. In Figure 5, we show the stacked seismic datasets that are used for the estimation of EI of different incidence angles.

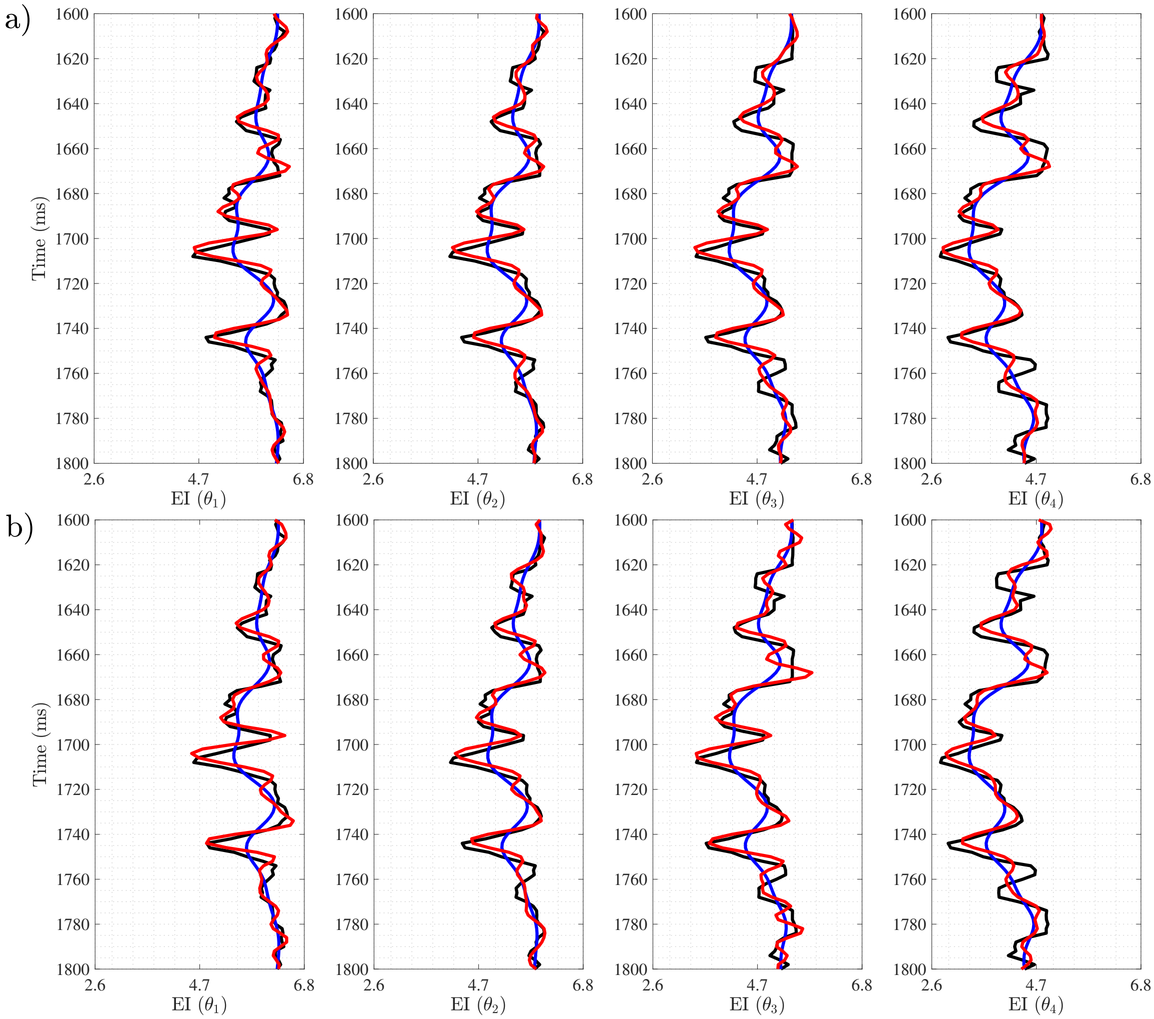

FIG. 3. Comparisons between true values (Black) and inversion results (Red) of EI of different incidence angles. a) Signal-to-noise ratio of 5; and b) Signal-to-noise ratio of 2. Blue curve represents the initial model of EI, which is a smoothed version of true value.

Using the DLS algorithm again, we implement the inversion for EI results of different incidence angles, which are used as the input for the estimation of reservoir parameters. In Figure 6, we show the inversion results of EI of incidence angles θ_1, θ_2, θ_3 and θ_4. We observe at locations where inversion results of EI exhibit low values the attached P-wave velocity also exhibits a relatively low value, which verifies the reliability of EI inversion results. Using the inversion results of EI, we implement the estimation of reservoir parameters.

In Figure 7, we show the final inversion results of V_c, ϕ, K_f and ρ, which are average values calculated using reservoir parameters estimated from EI results of different incidence angles.

At the location of gas-bearing reservoirs (around CDP 310 and Time 1450 ms), we observe that inversion results of V_c, K_f and ρ show relatively low values and inversion

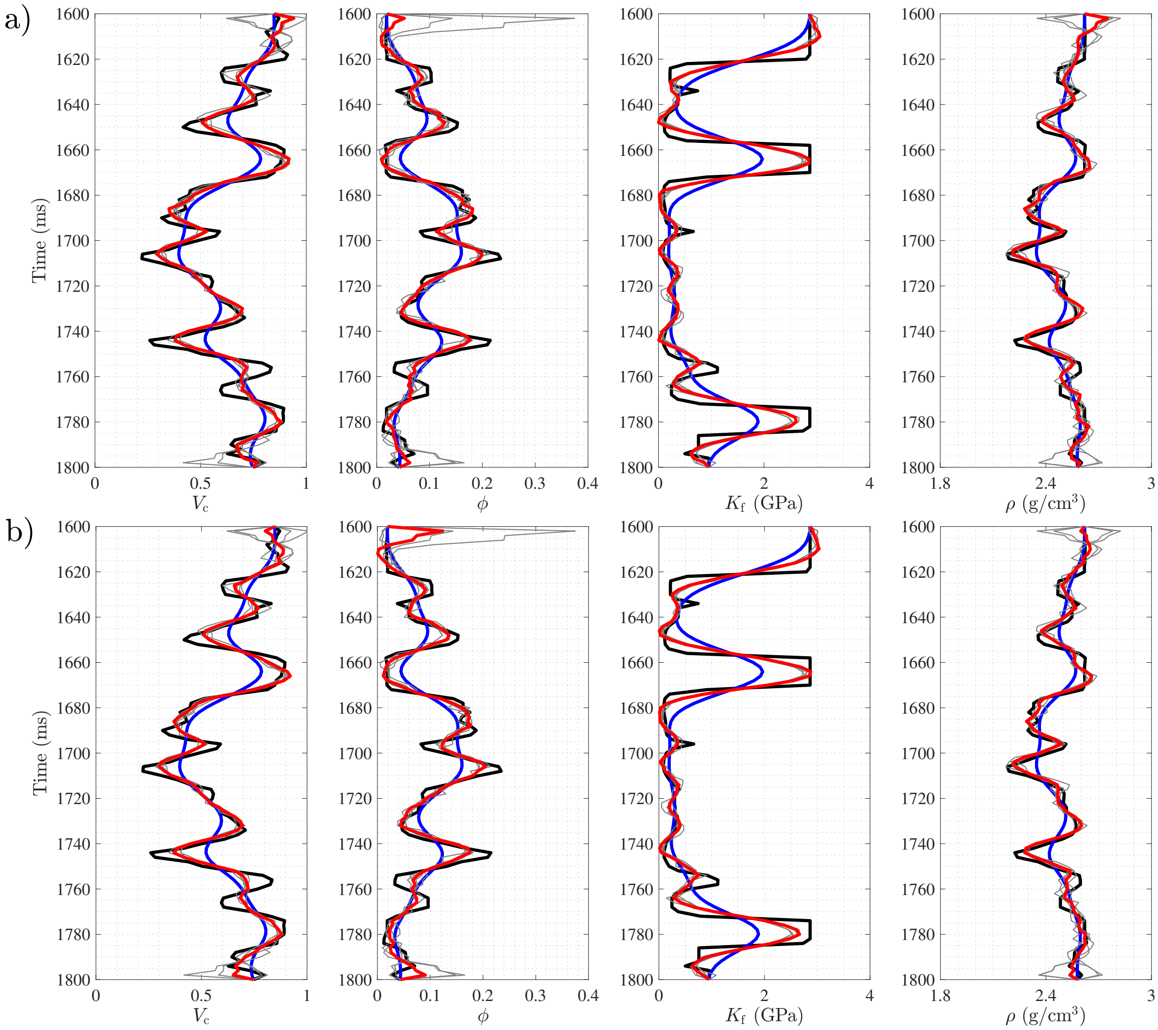

FIG. 4. Comparisons between true values (Black) and inversion results (Red) of shale content, porosity, fluid bulk modulus and density. a) Signal-to-noise ratio of 5; and b) Signal-to-noise ratio of 2. Blue curve represents the initial model of EI, which is a smoothed version of true value, and gray curve represents the inversion result that obtained using EI of each angle.

result of ϕ exhibits relatively high values, which may match the well log interpretation data. It validates that inversion results of reservoir parameters obtained using the proposed method are reliable and can be used for identifying hydrocarbon reservoirs.

CONCLUSION

Estimation of reservoir porosity, shale content and fluid type plays an important role in geophysical exploration. Based on petrophysical theory and equivalent models, the relationship between seismic wave reflection and reservoir porosity, shale content and fluid is constructed. Combining fluid substitution model and the average model, we first present the nonlinear reflection coefficient and elastic impedance (EI) that are expressed as a function of porosity, shale content, fluid bulk modulus and density; and using the derived reflection coefficient and EI, we propose a two-step inversion method, which involves: 1) using partially incidence-angle-stacked seismic data to implement a linear inversion to predict EI datasets; 2) using the predicted EI datasets to implement a nonlinear inversion for

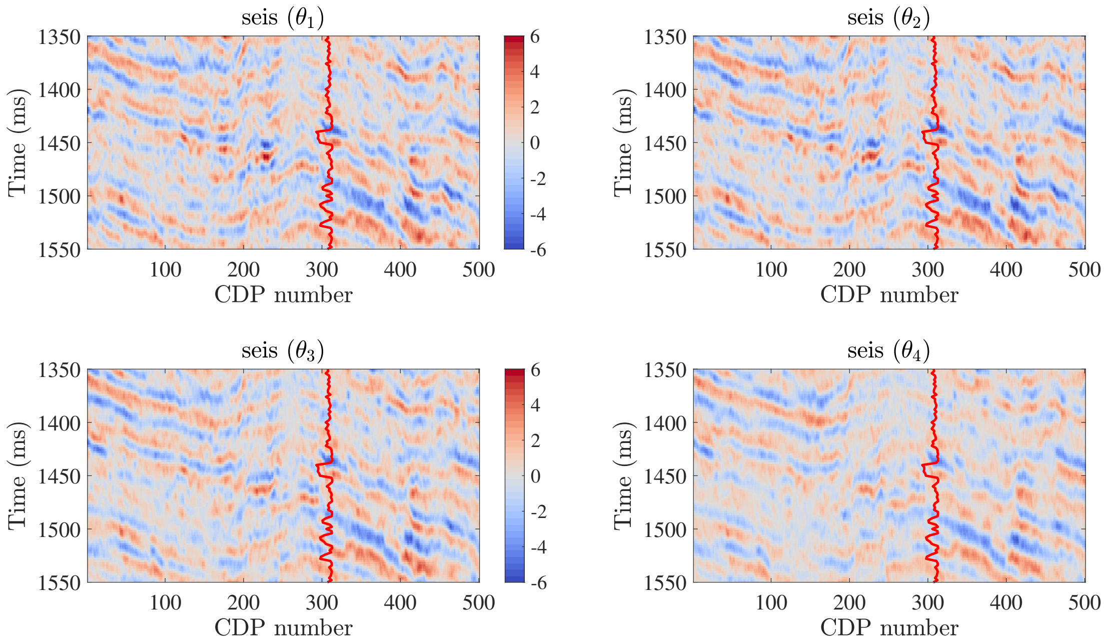

FIG. 5. Partially incidence-angle-stacked seismic data of angles of incidence $\theta_1 = 5°$, $\theta_2 = 12°$, $\theta_3 = 19°$ and $\theta_4 = 26°$. The curve represents P-wave velocity provided by well logging data.

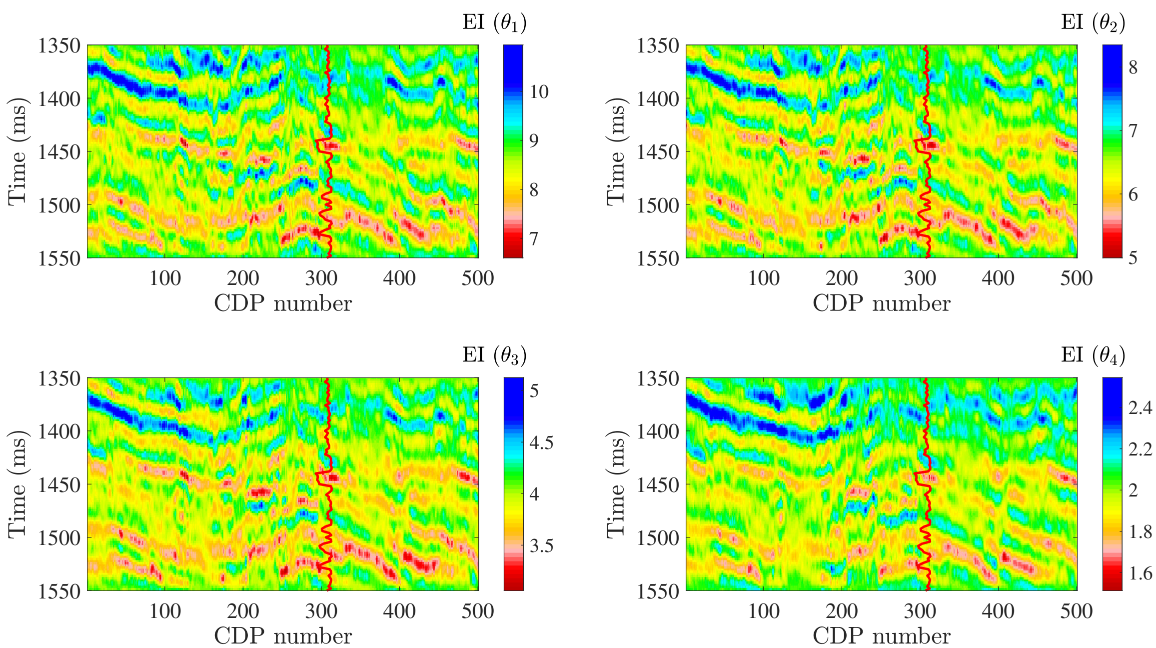

FIG. 6. Inversion results of EI of angles of incidence $\theta_1 = 5°$, $\theta_2 = 12°$, $\theta_3 = 19°$ and $\theta_4 = 26°$. The curve represents P-wave velocity provided by well logging data.

shale content, porosity, fluid modulus and density, during which we compute the first- and second-order derivatives of EI with respect to unknown parameters to improve the accuracy of inversion. The robustness of the proposed inversion method is verified using noisy seismic data. Applying the proposed method to real data, we may obtain reliable inversion results of reservoir parameters that can match the well log interpretation data.

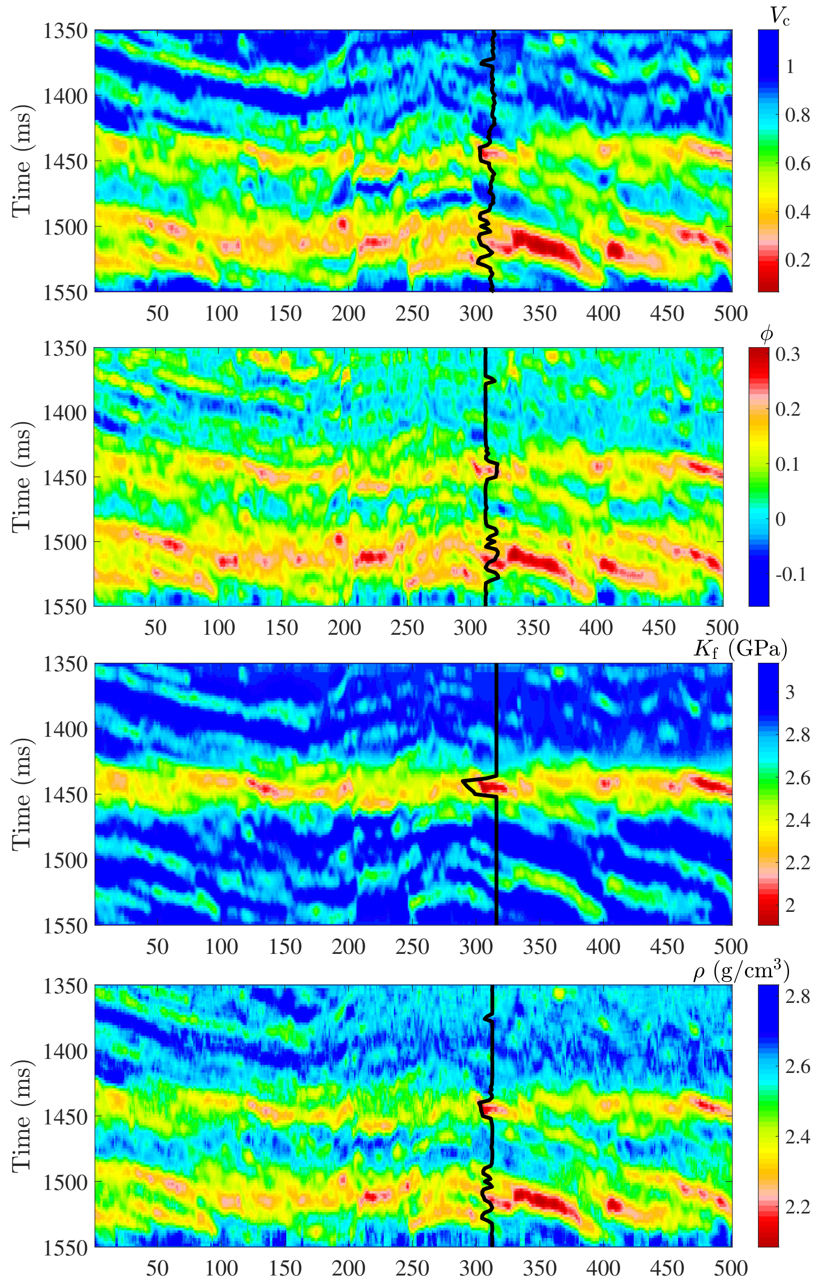

FIG. 7. Final inversion results of shale content, porosity, fluid bulk modulus and density. The curve represents the corresponding shale content, porosity, fluid bulk modulus and density provided by well log interpretation data.

ACKNOWLEDGMENTS

We thank the sponsors of CREWES for continued support. This work was funded by CREWES industrial sponsors, and NSERC (Natural Science and Engineering Research Council of Canada) through the grant CRDPJ 461179-13.

REFERENCES

Aki, K., and Richards, P. G., 1980, Quantitative seismology: University science books.

Chen, H., Li, J., and Innanen, K. A., 2020, Nonlinear inversion of seismic amplitude variation with offset for an effective stress parameter: Geophysics, **85**, No. 4, R299–R311.

Chen, H., and Zhang, G., 2017, Estimation of dry fracture weakness, porosity, and fluid modulus using observable seismic reflection data in a gas-bearing reservoir: Surveys in Geophysics, **38**, No. 3, 651–678.

Gassmann, F., 1951, Über die elastizität poröser medien: Vier. der Natur. Gesellschaft Zürich, **96**, 1–23.

Goodway, B., Chen, T., and Downton, J., 1997, Improved AVO fluid detection and lithology discrimination using lamé petrophysical parameters;"$\lambda\rho$","$\mu\rho$", & "λ/μ fluid stack", from P and S inversions, *in* SEG technical program expanded abstracts 1997, Society of Exploration Geophysicists, 183–186.

Gray, D., Goodway, B., and Chen, T., 1999, Bridging the gap: Using AVO to detect changes in fundamental elastic constants, *in* SEG Technical Program Expanded Abstracts 1999, Society of Exploration Geophysicists, 852–855.

Krief, M., Garat, J., Stellingwerf, J., and Ventre, J., 1990, A petrophysical interpretation using the velocities of P and S waves (full-waveform sonic): The Log Analyst, **31**, No. 06.

Russell, B. H., Gray, D., and Hampson, D. P., 2011, Linearized avo and poroelasticity: Geophysics, **76**, No. 3, C19–C29.

Russell, B. H., Hedlin, K., Hilterman, F. J., and Lines, L. R., 2003, Fluid-property discrimination with AVO: A Biot-Gassmann perspective: Geophysics, **68**, No. 1, 29–39.